Original Research

2-Bromopalmitate inhibits malignant behaviors of HPSCC cells by hindering the membrane location of Ras protein

Chen Wang[1], Zhao-Yang Cui[1], Hai-Yan Chang[2], Chang-Zhen Wu[1], Zhao-Yan Yu[1], Xiao-Ting Wang[1], Yi-Qing Liu[1], Chang-Le Li[1], Xiang-Ge Du[2] and Jian-Feng Li[1,3,4]

[1]Department of Otorhinolaryngology Head and Neck Surgery, Shandong Provincial Hospital, Shandong University, Jinan 250021, China; [2]Shandong Provincial Hospital, Shandong University, Jinan 250021, China; [3]Institute of Eye and ENT, Shandong Provincial Hospital, Shandong University, Jinan 250021, China; [4]Central Laboratory, Shandong Provincial Hospital, Shandong University, Jinan 250021, China

Corresponding authors: Jian-Feng Li. Email: LiJF@email.sdu.edu.cn; Xiang-Ge Du. Email: duxiangge@126.com

Impact Statement

For the first time, we found that DHHC9 and DHHC15, two PATs that mediate the palmitoylation of proteins, are more highly expressed in HPSCC tissues than in normal hypopharyngeal mucosae. Our further study demonstrated that at appropriate concentration, 2BP, a small-molecular inhibitor of protein palmitoylation, was able to inhibit the malignant biological behaviors of HPSCC cells without increasing cell apoptosis, possibly via hindering the palmitoylation and membrane location of Ras protein and interfering with FGF/ERK signaling transduction. From a new perspective of mechanism, 2BP is expected to be developed as a low-toxicity anti-HPSCC drug targeting Ras palmitoylation and membrane localization.

Abstract

Palmitoylation, which is mediated by protein acyltransferase (PAT) and performs important biological functions, is the only reversible lipid modification in organism. To study the effect of protein palmitoylation on hypopharyngeal squamous cell carcinoma (HPSCC), the expression levels of 23 PATs in tumor tissues of 8 HPSCC patients were determined, and high mRNA and protein levels of DHHC9 and DHHC15 were found. Subsequently, we investigated the effect of 2-bromopalmitate (2BP), a small-molecular inhibitor of protein palmitoylation, on the behavior of Fadu cells in vitro (50 μM) and in nude mouse xenograft models (50 μmol/kg), and found that 2BP suppressed the proliferation, invasion, and migration of Fadu cells without increasing cell apoptosis. Mechanistically, the effect of 2BP on the transduction of BMP, Wnt, Shh, and FGF signaling pathways was tested with qRT-PCR, and its drug target was explored with western blotting and acyl-biotinyl exchange assay. Our results showed that 2BP inhibited the transduction of the FGF/ERK signaling pathway. The palmitoylation level of Ras protein decreased after 2BP treatment, and its distribution in the cell membrane structure was reduced significantly. The findings of this work reveal that protein palmitoylation mediated by DHHC9 and DHHC15 may play important roles in the occurrence and development of HPSCC. 2BP is able to inhibit the malignant biological behaviors of HPSCC cells, possibly via hindering the palmitoylation and membrane location of Ras protein, which might, in turn, offer a low-toxicity anti-cancer drug for targeting the treatment of HPSCC.

Keywords: 2-Bromopalmitate, hypopharyngeal squamous cell carcinoma, malignant behaviors, protein palmitoylation, Ras protein, FGF/ERK signaling pathway

Experimental Biology and Medicine **2023; 248: 2393–2407. DOI: 10.1177/15353702231220671**

Introduction

Post-translational modification is the premise and basis for the biological activity and function of proteins.[1,2] Palmitoylation is an important lipid modification after protein translation and, also, is the only reversible lipid modification in organism. It is of great significance in the aggregation, structure stability, interconnection, transport, and localization of proteins.[3–6] In the past decade, with the discovery and research of PAT, the biological function of protein palmitoylation has gradually been studied in detail.

It has been found that there are 23 kinds of PAT in mammals, and these PAT proteins are called the DHHC protein family because they contain the zinc finger-like cysteine-rich domains, which are related to their acyltransferase activity.[7] At first, the studies found that the protein palmitoylation mediated by DHHC proteins played a role in virus invasion and parasite activity.[8,9] Subsequently, the deeper study

revealed that the function of DHHC proteins was significantly related to animal embryonic development. In previous studies, it has been found that palmitoylation mediated by DHHC proteins is involved in stem cell proliferation, differentiation, self-renewal, and other aspects. For example, DHHC13 regulates the proliferation of embryonic stem cells, as well as the differentiation of ectoderm and mesoderm,[10] DHHC16 promotes the self-renewal of telencephalic neural stem cells,[11] DHHC5 regulates the differentiation of retinal cells,[12] and DHHC15 affects the differentiation of neural stem cells.[13]

Stem cells and tumor cells are highly consistent in biological activities such as proliferation, differentiation, migration, gene expression, and activation of regulatory molecules. The concept of cancer stem cells (CSC) has been proposed and generally accepted by the academic community.[14,15] With the continuous revelation of the roles of DHHC proteins in the field of stem cells, their function on tumor occurrence and progression has gradually attracted attention in recent years. Researchers began to study the role and mechanism of some members of DHHC proteins in the proliferation, metastasis, and apoptosis of tumor cells.[16–18] However, the role of these proteins in different tumors is different, and the role of some members has not reached consensus. At present, the tumor-related research on protein palmitoylation is mainly limited to the mechanism research on single DHHC member. The research on tumor treatment methods, which are related to protein palmitoylation has not yet started, and there is still no systematic report on related drug development in this field.

Small-molecular compounds have the advantages of high permeability, strong reversibility and easy synthesis, which are currently the best choice for cell intervention and drug screening. 2BP, a small-molecular inhibitor of protein palmitoylation, possesses a structure highly similar to that of saturated palmitic acid. It can competitively bind with DHHC-CRD of DHHC protein, thereby inhibiting the activity of PAT enzyme and reducing the palmitoylation level of protein.[19] Considering the roles of DHHC proteins in tumor stem cells, we speculated that 2BP might affect the occurrence and progression of tumor cells.

HPSCC is a common pathological type of head and neck tumor, whose prognosis is very poor. At present, surgery is still the main treatment method for HPSCC, which can be combined with adjuvant radiotherapy and chemotherapy. However, there is no particularly ideal chemotherapy drug at present, resulting in a 5-year survival rate of only 30% to 54% for HPSCC patients in stage III–IV.[20,21] To date, despite the roles of DHHC proteins that have been elucidated in different types of tumors, their status and effect in HPSCC tissues have been studied sparingly. Therefore, the present study was initially designed to analyze the difference in the expression levels of 23 kinds of DHHC proteins between human normal hypopharyngeal mucosal tissues and this kind of tumor, so as to search for potential tumor markers relevant to protein palmitoylation in HPSCC. Then, the effect of 2BP on the proliferation, apoptosis, migration, and invasion of HPSCC *in vivo* and in nude mouse xenograft models was studied, with special attention given to the molecular mechanism underlying such actions of 2BP.

Materials and methods

Patients and tissue samples

The tissue samples were resected from patients with hypopharyngeal carcinoma, who were treated by surgery in Shandong Provincial Hospital. After resection, the tumor tissue was confirmed as HPSCC by pathological analysis. At the same time, the tissues at the cutting edge were separated from the specimen and taken for pathological examination to confirm that there were no tumor cells in them. The normal mucosa of the cutting edge and the tumor-bearing tissue were taken for assays.

Cell culture

The human HPSCC cell line (Fadu) was obtained from the Cell Bank of the Chinese Academy of Sciences (Shanghai, China) and stored in liquid nitrogen. Cells were cultured in Dulbecco's modified Eagle's medium (DMEM) containing 10% fetal bovine serum (FBS; Gibco, USA) and grown in a humidified incubator at 37°C with 5% carbon dioxide. Before each experiment, cells were seeded in new culture plates and incubated to appropriate density. Then, cells were treated with 2BP (Sigma-Aldrich Co. LLC) at appropriate concentrations or blank culture solution. At the corresponding time points, the cells were collected for assays.

Xenograft studies in BALB/c nude mice

Male BALB/c nude mice were obtained from Vital River Laboratories (Beijing, China) and maintained in accordance with Chinese animal welfare requirements. They were randomly divided into control group and 2BP-treated group when they were 7-week-old (weighing 25–30 g). 0.1 mL Fadu cells (1×10^5 mL) were subcutaneously injected into the right flank of each mouse. When the maximum diameter of the established tumor reached 3–5 mm, the 2BP-treated group received intraperitoneal injection of 2BP (50 μmol/kg), and the control group received the same amount of vehicle (0.5% DMSO) every 24 h. The treatment continued for 21 days. Body weight and tumor volume were measured every three days. Tumor volumes were calculated with the formula: $V = (\text{min diameter})^2 \times (\text{max diameter})/2$.[22] After 21 days, mice were euthanized under anesthesia, and the tumor specimens were harvested, weighed, and then processed for protein analysis. The animal experiments were conducted in compliance with the ARRIVE guidelines.

RNA isolation and quantitative real-time polymerase chain reaction (qRT-PCR)

Total RNA was extracted from tissue samples or harvested Fadu cells with Trizol reagent (Invitrogen). RevertAid™ First Strand cDNA Synthesis Kit (Thermo Fisher Scientific Inc.) was used for reverse transcription according to the manufacturer's instructions. qRT-PCR with iQSybr Green Supermix (Bio-Rad Laboratories, Inc.) was performed with qTOWER 2.0 (Analytik Jena AG, Germany). Delta-delta CT method was used for calculation of transcription levels, and β-actin served as the normalization control. Each assay was done in triplicate. Primers for PCR are listed in Table 1.

MTT (3-(4,5-dimethylthiazol2-yl)-2,5-diphenyltetrazolium bromide) assay

Cell viability was assessed by adding MTT (Sartorius Corporation) to the cell cultures (0.5 mg/mL). Cells were incubated at 37 °C for 1 h, and the medium was removed. Then, we added dimethyl sulfoxide (Sartorius Corporation) to each well. The absorbance value at 490 nm of each well was quantified with a multi-well spectrophotometer (Bio-Rad Laboratories, Inc.) immediately. Three independent experiments were done.

Protein extraction and western blotting

Total protein extraction was performed as previously described.[23] Briefly, cells or tissues were lysed in radioimmunoprecipitation assay buffer with protease-inhibitor cocktail, phosphatase inhibitors, and phenyl-methyl-sulfonyl fluoride for 30 min and then centrifuged (12,000 rpm) at 4 °C for 15 min. Supernatants were then collected. Cell membrane protein was extracted with a membrane and cytosol protein extraction kit (Beyotime Biotechnology) according to the instruction manual. Bicinchoninic acid assay (Beyotime Biotechnology) was used for protein concentration detection. Equal amounts of protein samples were separated by 10% SDS-polyacrylamide gel electrophoresis and then transferred to a polyvinylidene fluoride membrane. In Tris-buffered saline with Tween-20 (TBST), the membranes were blocked with 5% milk and incubated with primary and secondary antibodies sequentially. The membranes were washed with TBST and then developed with ECL detection system. The intensity of bands was measured with Image J Software. Primary antibodies used in the study were anti-DHHC9 antibody (1:500; Abcam plc), Anti-DHHC15 antibody (1:200; Abcam plc), anti-β-actin antibody (1:1000; Sigma-Aldrich Co. LLC), anti-PCNA antibody (1:1000; Abcam plc), Anti-Ki-67 antibody (1:1000; Abcam plc), anti-caspase3 antibody (1:1000; Cell Signaling Technology, Inc.), anti-cleaved-caspase3 antibody (1:1000; Cell Signaling Technology, Inc.), anti-MMP2 antibody (1:1000; Abcam plc), anti-MMP9 antibody (1:1000; Abcam plc), anti-Ras antibody (1:1000; Abcam plc), anti-t-ERK1/2 antibody (1:1000; Cell Signaling Technology), anti-p-ERK1/2 antibody (1:1000; Cell Signaling Technology), and anti-NaK ATPase α1 antibody (1:1000; Abcam plc).

Terminal deoxynucleotidyl transferase-mediated dUTP nick-end labeling (TUNEL) assay

As described in the manufacturer's instructions, an *in situ* cell death detection kit (Promega, Madison, WI, USA) was used for TUNEL assay. Then, the calculation of the percentages of TUNEL-positive cells was conducted with a fluorescence microscope (Olympus IX71).

5-Bromo-2-deoxyuridine (Brdu) labeling assay

Fadu cells were plated on poly-l-lysine-coated glass coverslips and Brdu (10 μM, Sigma-Aldrich) was added to the medium and incubated for 2 h. After fixation, cells were immunostained with anti-Brdu antibody (1:1000; Sigma-Aldrich) and observed with a fluorescence microscope (Olympus IX71). Percentages of Brdu positive cells were calculated.

Flow cytometry analysis

Fadu cells were trypsinized and then collected by centrifugation. After resuspension, they were washed with PBS and fixed with 75% ethanol at room temperature for 1 h. Then, the fixed cells were incubated in 20 μg/mL propidium iodide and 10 mg/mL RNase A for 30 min. The cell cycle distribution analysis was conducted with FC500 flow cytometer (Beckman Coulter).

Acyl-biotinyl exchange (ABE) assay

As previously described, the palmitoylation level of protein was determined by ABE assay.[23] Briefly, the protein samples were incubated with N-ethylmaleimide (50 mM, Thermo Fisher Scientific Inc.) to block the free sulfhydryl groups and immunoprecipitated with anti-Ras antibody (2 μg). Then purified samples were treated with or without hydroxylamine (1M, room temperature, Thermo Fisher Scientific Inc.) and biotin-BMCC (0.5 μM, 4°C, Thermo Fisher Scientific Inc.) for 1 h, respectively, to label the palmitoylated sites. After sodium dodecyl sulfate-polyacrylamide gel electrophoresis, the amount of biotin on Ras proteins was determined with horseradish peroxidase-conjugated streptavidin (SA-HRP, Beyotime Biotechnology).

Wound-healing assay

Briefly, Fadu cells were seeded in a six-well plate and incubated to 90% confluency. In the monolayer cells, a scratch was created with a 10-μL pipette. Then, cells were incubated in the culture medium with or without 50 μM 2BP. After 0 and 48 h, Photographs at the same site were taken and the migration areas were measured and analyzed with ImageJ software.

Transwell assay

As previously described, transwell invasion and migration assay were conducted with a transwell culture chamber system.[24] Briefly, 1×104 Fadu cells were seeded in the upper chamber containing serum-free culture medium with or without 50 μM 2BP. In the lower chamber, 600 μL FBS-containing DMEM (10%) was added. Filter membrane with 8 μm pores was between the upper and lower chamber. For invasion assay, the filter membrane was precoated with matrigel (BD Biosciences, USA), while for the migration test, it was not. After incubation for 48 h, the cells attached to the upper side of the fibrous membrane were gently removed, while the cells under the fibrous membrane were fixed and then stained with 0.1% crystal violet for 8 min. The stained cells were photographed and counted with an IX71 microscope (Olympus).

Data analyses

Quantitative data were presented as mean ± standard error of the mean (SEM). At least three independent experiments

Table 1. Primers for qRT-PCR.

Gene	Primer sequence (5'–3')	
dhhc1	Sense primer	GGCTTTGGGATCCTTGTTCC
	Anti-sense primer	TCACATCCACGTTGCACAAG
dhhc2	Sense primer	CTCGGCTGGTCCTACTACG
	Anti-sense primer	GGCTTCTCCTCTTGGCTCT
dhhc3	Sense primer	TGTTCCTCTCTTTGGCCCAT
	Anti-sense primer	CTGCACCTCCAAACACTGAC
dhhc4	Sense primer	CACCTTCATTGTCCTGCACC
	Anti-sense primer	TTGGTTCCACAAGTCAGGGT
dhhc5	Sense primer	CGAGCTGAGGAGGATGAGG
	Anti-sense primer	TCCGGCGACCAATACAGTT
dhhc6	Sense primer	GTCCCATCATAGCCCTTGGT
	Anti-sense primer	GGACCGACAAACATGGCATT
dhhc7	Sense primer	CTGTGCTGTCATGACGTGG
	Anti-sense primer	TTTCAGGGTCGGTGAGCAT
dhhc8	Sense primer	GGATGAGAAGCCACTGGACT
	Anti-sense primer	CTTGTACATGGCAGGTGTCG
dhhc9	Sense primer	TTTACACTCTGGTCCGTCGT
	Anti-sense primer	CACAGCACTTCACAGCAGTT
dhhc11	Sense primer	CTCCCTGCTGATTCACAAGC
	Anti-sense primer	CATCTGCTTCCTGTGCCATC
dhhc12	Sense primer	TTCATCTCCTCACACCGCAT
	Anti-sense primer	TGGTTTTCAGGCACAAGACG
dhhc13	Sense primer	TGTGTCGCTTCTTCATTGGG
	Anti-sense primer	CAGGTGGATGCTGCTGAATC
dhhc14	Sense primer	CAAGTGTCTGTGCTGTGTCC
	Anti-sense primer	TTTCTGTCAGGAGCCTCTCG
dhhc15	Sense primer	CCAGTGTTTACAAGTGGCCC
	Anti-sense primer	ATCCTCGTTGTCTTCCCAGG
dhhc16	Sense primer	TTGGAGTGGTGTTCGTGGT
	Anti-sense primer	GTGGTGATGGCCTGGTAGT
dhhc17	Sense primer	CATTGGGCAGTGCTAGCAG
	Anti-sense primer	TTGCTTGCCTTGCCTCTTG
dhhc18	Sense primer	CTTCTTCGTCATGAGCTGCC
	Anti-sense primer	CTTCAGCTTCACCATCTGCC
dhhc19	Sense primer	GCTGGTCACCTGTCTCATCT
	Anti-sense primer	TGGTCGAAGGGGTTGTATCC
dhhc20	Sense primer	TTTTCCAACTCGCCTTGTGG
	Anti-sense primer	GACGATGCCTTCTTCAGCTC
dhhc21	Sense primer	TGCAAGCTAATTTGGCCACAT
	Anti-sense primer	GATCTTCACTTGGCTCTGCTG
dhhc22	Sense primer	CCATGAGGGTTGTTTGGGTTT
	Anti-sense primer	GAGATGCACAAGAAGTAGGCG
dhhc23	Sense primer	GTCGGGCAGTCTCAACAATC
	Anti-sense primer	TCCTCACACAGATGCCACAT
dhhc24	Sense primer	CAATCCATGTCCTGCCACAG
	Anti-sense primer	TGCCTGCAAATCACTGTTCC
cxxc5	Sense primer	CTGGGCAAAGAATGGACAAT
	Anti-sense primer	TGGTCGGAAAGAATCAAAGG
gata2	Sense primer	CCCCACCTACCCCTCCTAT
	Anti-sense primer	CTGCCCATTCATCTTGTGG
myc	Sense primer	CATGCCTTGGTTCATCTGG
	Anti-sense primer	TTTGTGTGCCTCAGCTTCC
ccnd1	Sense primer	TTGAGGGACGCTTTGTCTG
	Anti-sense primer	GGTGCAACCAGAAATGCAC
ptch1	Sense primer	TCAGCAATGTCACAGCCTTC
	Anti-sense primer	GTCGTGTGTGTCGGTGTAGG
nkx2-2	Sense primer	GTGGCTTGTTTGGGTTTGTT
	Anti-sense primer	CCGAATAGCTGAGCTCCAAG
etv4	Sense primer	TCATTGGGAAGGAAAAGTGG
	Anti-sense primer	GAGATCTGGGGAGCTCAGTG
etv5	Sense primer	TTGTGCTTTCTGCACCAGAC
	Anti-sense primer	TGACCAGGTTTCCAAAGGAC
fgf1	Sense primer	CTGCAGTAGCCTGGAGGTTC
	Anti-sense primer	GGCTGTGAAGGTGGTGATTT
fgf2	Sense primer	TGGTGAAACCCCGTCTCTAC
	Anti-sense primer	TCTGTTGCCTAGGCTGGACT
fgf3	Sense primer	GGATAACCTGGAGCCCTCTC
	Anti-sense primer	GCTGGCTCTGGAAATAGCTG
fgf8	Sense primer	TCATCCGGACCTACCAACTC
	Anti-sense primer	CTCCTCGGACTCGAACTCTG

were done for each assay. Statistical analysis of data was carried out by Student's *t*-tests to compare the differences between groups. When the *P*-values < 0.05, the difference was considered statistically significant (ns: $P > 0.05$; *: $P < 0.05$; **: $P < 0.01$; ***: $P < 0.001$; ****: $P < 0.0001$).

Results

DHHC9 and DHHC15 were highly expressed in HPSCC tissues

Before studying the pharmacological effects of 2BP, we first detected and compared the transcription levels of all 23 PATs in tumor tissue and normal mucosa of 8 patients with HPSCC using qRT-PCR. Among them, the mRNA expression levels of DHHC1, DHHC7, DHHC11, DHHC19, and DHHC22 could not be detected in both groups of tissues (CT value > 35). The mRNA expression levels of DHHC2, DHHC3, DHHC4, DHHC5, DHHC6, DHHC8, DHHC12, DHHC13, DHHC14, DHHC16, DHHC17, DHHC18, DHHC20, DHHC21, DHHC23, and DHHC24 were not significantly different between the two groups, whereas the transcription levels of DHHC9 and DHHC15 in tumor tissue were significantly higher than those in normal mucosa (Figure 1(A)). Besides, the increased protein levels of DHHC9 and DHHC15 in HPSCC tissues were also confirmed by western blotting (Figure 1(B)).

2BP inhibited the proliferation of HPSCC cells

We used the MTT method to preliminarily determine the effect of 2BP with different concentration gradients (1-100 μM) on the viability of Fadu cells. When the drug concentration of 2BP was below 50 μM, the cell viability continued to increase within 72 h after drug treatment. During this process, as the concentration of 2BP increased, the growth rate of cell viability decreased. When the drug concentration was above 62.5 μM, the cell viability began to show negative growth over time, and the higher the drug concentration, the faster the negative growth (Figure 2(A)). After careful consideration, we selected 50 μM as our subsequent experimental concentration because it inhibited the growth of HPSCC cells, but its low cytotoxicity could still ensure enough cell viability for future research.

Subsequently, we used the Brdu labeling assay to detect the effect of 2BP on the proliferation of Fadu cells. The results

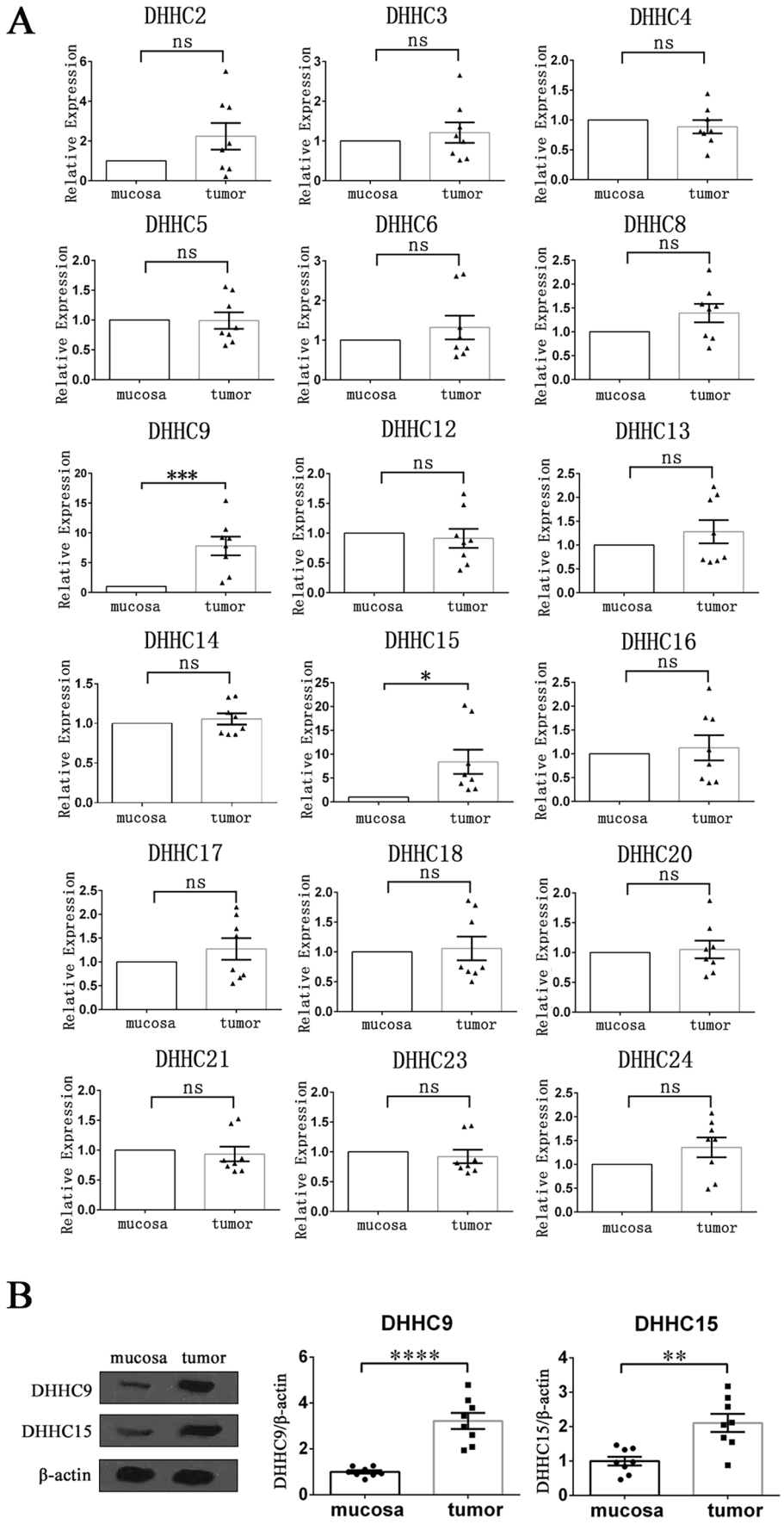

Figure 1. Expression levels of PATs in HPSCC tumor tissues and normal mucosa tissues. (A) qRT-PCR was performed to detect and compare the mRNA expression levels of PATs (DHHC protein family) in tumor tissues and normal mucosal tissues of 8 HPSCC patients. β-actin acted as an internal control. Data were shown as mean ± SEM. (B) The protein expression levels of DHHC9 and DHHC15 in tumor tissues and normal mucosal tissues of 8 HPSCC patients were determined with western blotting. The gray value of each strip was detected by Image J software. β-actin acted as an internal control. Standardized data were shown as mean ± SEM.

showed that after 48 h of drug treatment, the percentage of Brdu-positive cells in 2BP-treated group was significantly lower than that in the control group ($t = 5.095$, $P = 0.007$), indicating that 2BP could inhibit the proliferation of Fadu cells (Figure 2(B)). We further used flow cytometry to study the difference in the cell cycle distribution of Fadu cells between the 2BP-treated group and the control group, finding that after 48 h of 2BP treatment, the number of Fadu cells in G0/G1 phase significantly increased (2BP-treated group:75.58 ± 2.57%, control group: 48.48 ± 1.88%; $t = 8.527$, $P = 0.001$), while the proportion of cells in S phase (2BP-treated group:14.98 ± 1.83%, control group: 31.37 ± 2.56%; $t = 5.241$, $P = 0.007$) and G2/M phase (2BP-treated group: 9.44 ± 0.75%, control group: 20.14 ± 1.46%; $t = 6.525$, $P = 0.003$) significantly decreased (Figure 2(C)). These results demonstrated that 2BP could arrest the proliferation cycle of Fadu cells in the G0/G1 phase.

To validate our experimental results at the molecular level, we used western blotting to detect the expression levels of two important cell proliferation markers in Fadu cells. The experimental results showed that the expression levels of Ki-67 and PCNA in 2BP-treated Fadu cells were significantly lower than those in the control group at 24 and 48 h after drug treatment, confirming that 50 μM 2BP could significantly inhibit the proliferation of HPSCC cells *in vitro* (Figure 2(D)).

50 μM 2BP treatment did not significantly affect the apoptosis of HPSCC cells

The growth rate of tumors not only depended on the proliferation of tumor cells, but also on the cell apoptosis. We performed TUNEL assay to investigate the effect of 50 μM 2BP treatment on Fadu cell apoptosis. The results showed that after 48 h of drug treatment, there was no significant difference in the percentage of TUNEL positive Fadu cells between 2BP-treated group and control group ($t = 0.453$, $P = 0.674$; Figure 3(A)). At the molecular level, we used western blotting to detect the activation level of caspase3, which was the executing protein of cell apoptosis. The experimental results showed that there was no significant difference in the expression level of cleaved-caspase3 in Fadu cells between 2BP-treated group and control group at both 24 and 48 h after drug treatment (Figure 3(B)). These results indicated that 50 μM 2BP treatment did not significantly increase the apoptosis of HPSCC cells.

50 μM 2BP treatment inhibited the migration and invasion of HPSCC cells

We used wound-healing experiment to determine the effect of 50 μM 2BP treatment on Fadu cell migration. After drug treatment for 48 h, the migration area of Fadu cells in the 2BP-treated group was significantly smaller than that in the control group ($t = 4.102$, $P = 0.015$; Figure 4(A)). The transwell experiment also showed that after drug treatment, fewer cells in the 2BP-treated group could migrate through the fibrous membrane that was not coated with matrigel ($t = 6.065$, $P = 0.004$; Figure 4(B)), proving that 50 μM 2BP treatment could significantly inhibit the migration of Fadu cells. Besides, we also found that after drug treatment, the number of Fadu cells invading through the matrix-coated fibrous membrane in the 2BP-treated group was significantly lower than that in the control group ($t = 3.810$, $P = 0.019$; Figure 4(C)), indicating that 50 μM 2BP treatment could also reduce the invasive ability of HPSCC cells.

MMP2 and MMP9 were important markers that could reflect the tumor migrational and invasive ability at molecular level. After 50 μM 2BP treatment for 24 and 48 h, the expression levels of these two proteins in Fadu cells were detected using western blotting, and significantly reduced expression levels of MMP2 and MMP9 were found in 2BP-treated group (Figure 4(D)).

2BP suppressed the HPSCC growth and progression in nude mouse xenografts

In order to further validate the anti-cancer effect of 2BP *in vivo*, we constructed HPSCC nude mouse xenograft model. Fadu cells were implanted in the nude mice and subcutaneous tumors formed. Then, the mice were treated with 2BP (50 μmol/kg). During the drug treatment period, there was no significant difference in body weight between the 2BP-treated mice and the control mice (Figure 5(Ab)), but the growth rate of tumor volume in 2BP-treated group was slower than that in control group (Figure 5(Ac)). After 21 days, the mice were euthanized and the tumor tissues were resected (Figure 5(Aa)). The volume and weight of tumors isolated from 2BP-treated mice were significantly lower than those of the control group (Figure 5(Ad) and (Ae)).

Afterward, we extracted total proteins from the isolated tumor tissues of 2BP-treated group and control group. Using western blotting analysis, we detected the expression levels of marker proteins related to proliferation, apoptosis, invasion, and migration of tumor cells in two groups. Consistent with the results of experiments *in vitro*, the protein expression levels of Ki-67, PCNA, MMP2, and MMP9 in the 2BP-treated group were significantly higher than those in the control group, while the activation level of caspase3 was not significantly different compared to the control group (Figure 5(B)), demonstrating that 2BP could suppress the proliferation, migration and invasion of HPSCC cells, but not promote cell apoptosis *in vivo*.

2BP inhibited palmitoylation of Ras protein, hindered its membrane localization and interfered with FGF/ERK signaling transduction

In order to further investigate the underlying molecular mechanism, we determined the mRNA expression levels of several downstream target genes of important signaling transduction pathways involved in tumor cell proliferation, invasion and migration using qRT-PCR. No significant difference in the transcription levels of target genes of BMP signaling pathway (*cxxc5* and *gata2*), Wnt signaling pathway (*myc* and *ccnd1*), and Shh signaling pathway (*ptch1* and *nkx2-2*) between 2BP-treated Fadu cells and control cells was found. However, significantly reduced mRNA expression levels of *etv4* and *etv5*, which were directly regulated by FGF signaling pathway, were detected in 2BP-treated group (Figure 6(A)). Further experiments found that in the 2BP-treated group, the expression levels of *fgf1*, *fgf2*, *fgf3*, and *fgf8*, which were

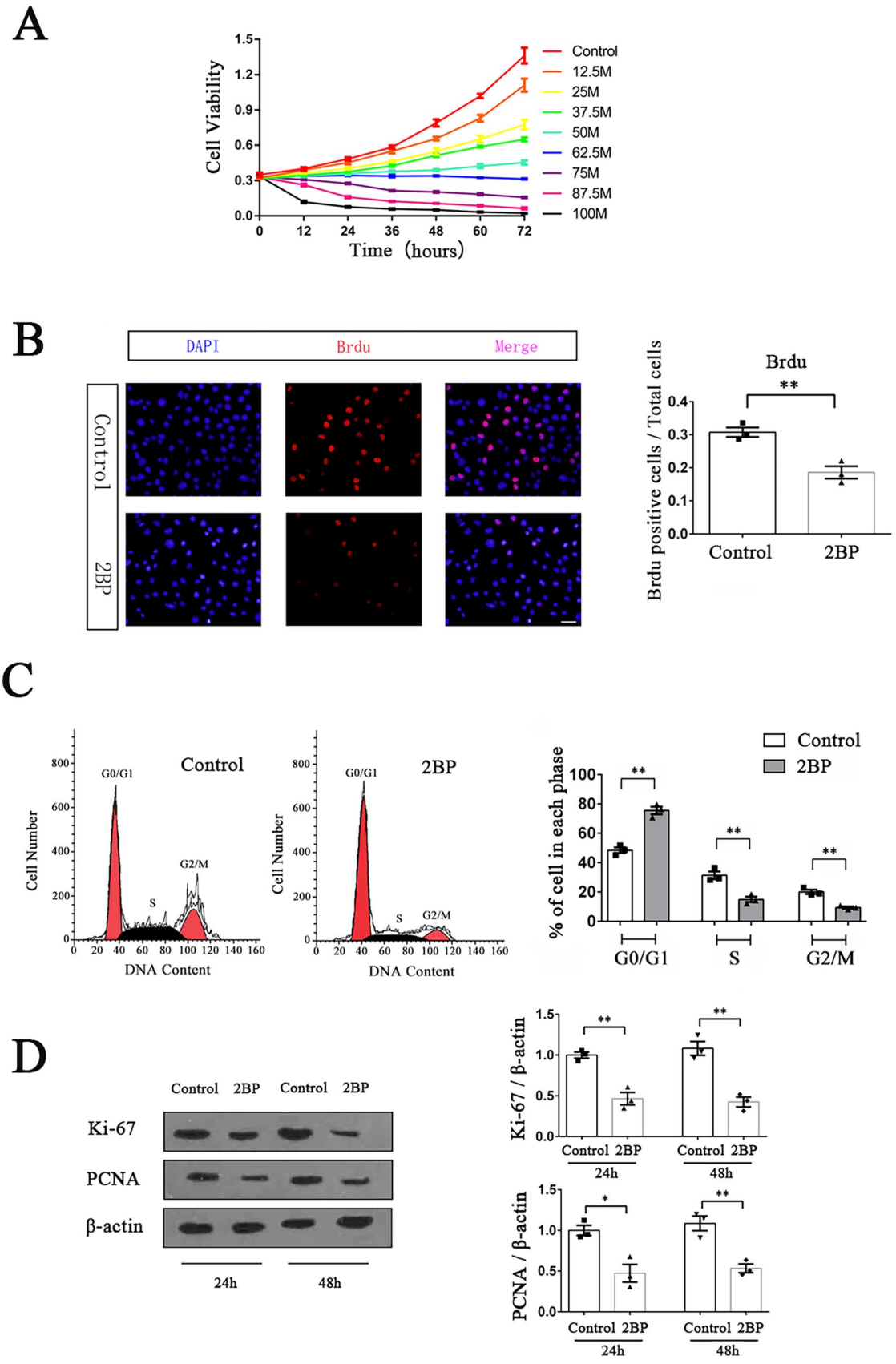

Figure 2. 2BP inhibited the proliferation of HPSCC cells. (A) MTT method was used to detect the cell viability of Fadu cells treated with different concentrations of 2BP in 72 h. Cell viability-time curves were drawn, and their slopes represented the cell growth rates. (B) Brdu labeling assay was performed to compare the proliferation of Fadu cells between the 2BP-treated group (50 μM) and the control group at 48 h after drug treatment. Scale bar represented 30 μm. Brdu positive cells (red)/total cells (blue) were calculated and shown as mean ± SEM. (C) The cell cycle distribution of Fadu cells at 48 h after drug treatment was determined with flow cytometry. Percentages of cells in G0/G1, S, and G2/M phase were shown as mean ± SEM. (D) The protein expression levels of Ki-67 and PCNA were determined with western blotting assay at 24 and 48 h after drug treatment. The gray value of each strip was detected by Image J software. β-Actin acted as an internal control. Standardized data were shown as mean ± SEM.

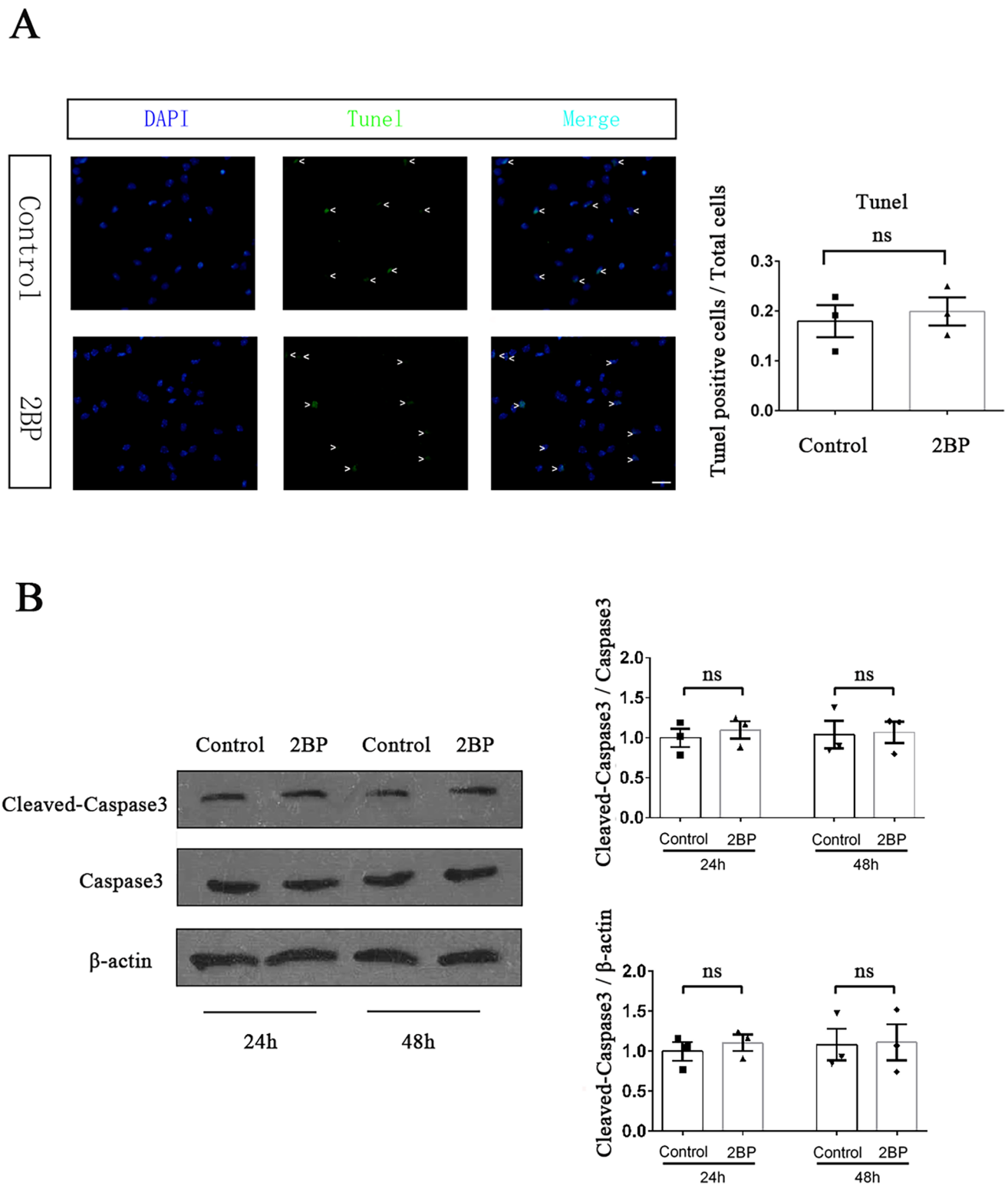

Figure 3. 50 μM 2BP did not increase the apoptosis of Fadu cells. (A) TUNEL assay was performed to compare the apoptosis of Fadu cells between the 2BP-treated group (50 μM) and the control group at 48 h after drug treatment. TUNEL positive cells (green)/total cells (blue) were calculated and shown as mean ± SEM. Scale bar represents 30 μm. (B) The protein expression level of cleaved-caspase3 was determined with western blotting assay at 24 and 48 h after drug treatment. The gray value of each strip was detected by Image J software. Capases3 and β-actin acted as internal control, respectively. Standardized data were shown as mean ± SEM.

important activators of the FGF signaling pathway, did not significantly change (Figure 6(B)). However, the phosphorylation level of ERK1/2, which was the key protein in the FGF signal transduction process, decreased significantly (Figure 6(C)), indicating that 2BP interfered with the transduction of FGF/ERK signaling pathway.

Subsequently, we studied the molecular structure of the key proteins upstream of ERK in the FGF/ERK signaling

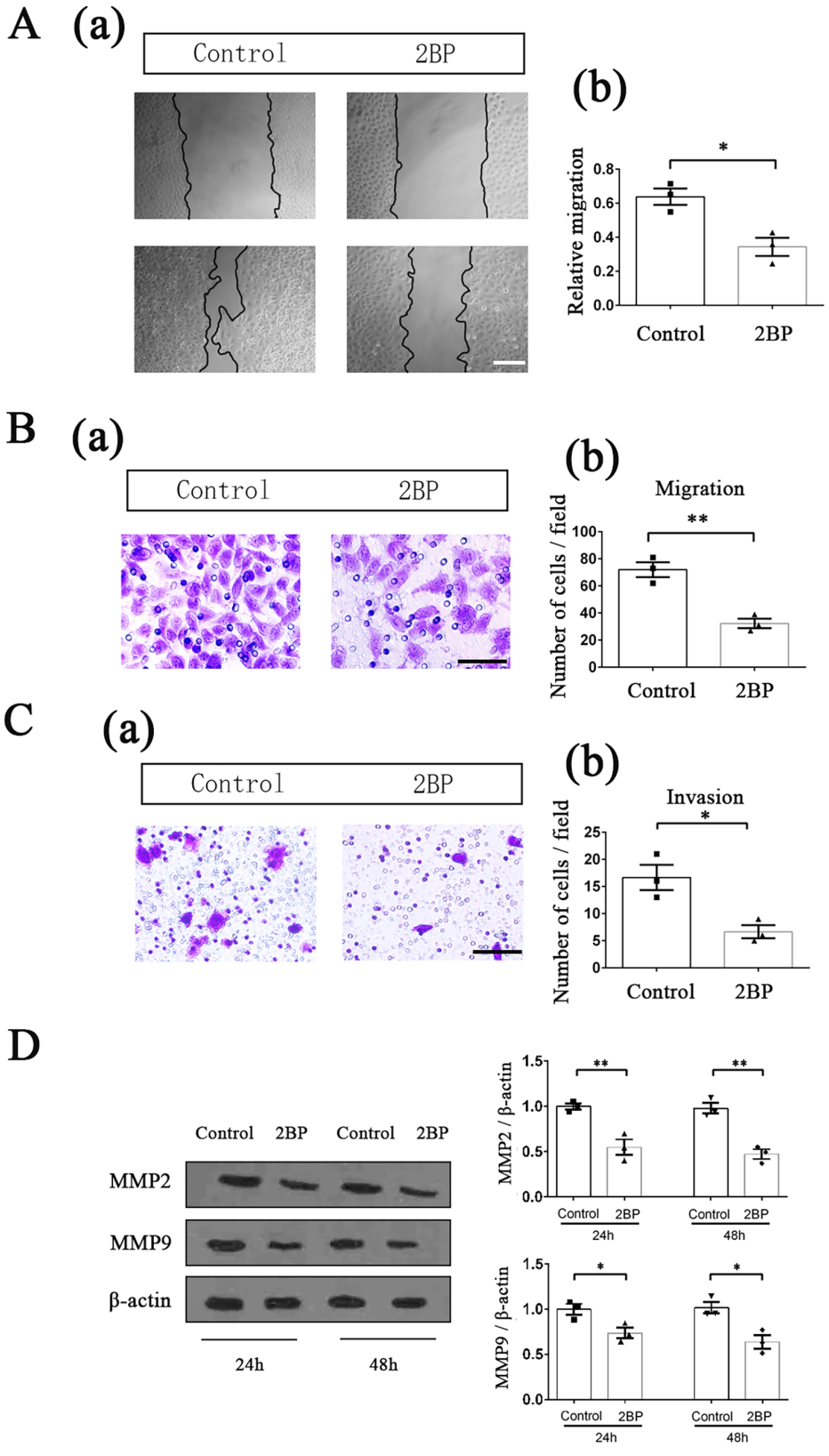

Figure 4. 50 μM 2BP inhibited the migration and invasion of HPSCC cells. Effect of 2BP on the migration of Fadu cells was tested by wound-healing experiment. (a) Fadu cells were scraped with a pipette tip and then incubated with or without 50 μM 2BP for 48 h. The area of the scratch was measured with the Image J software. Scale bar represents 100 μm. (b) Relative migration was quantified as (Initial scratch area—scratch area after 48 h)/Initial scratch area. Data were shown as mean ± SEM. (B) Effect of 2BP on migration of Fadu cells was tested by transwell system in which the fibrous membrane was not coated with matrigel. (a) Migrational cells on the bottom side of the membrane were photographed and counted after 50 μM 2BP treatment for 48 h. Scale bar represented 30 μm. (b) Quantification of migrational cells. The migrational cells were counted in 10 different fields, and the average was calculated. Data were presented as mean ± SEM. (C) Effect of 2BP on invasion of Fadu cells was tested by matrigel-coated transwell system. (a) Invasive cells on the bottom side of the membrane were photographed and counted after 50 μM 2BP treatment for 48 h. Scale bar represents 60 μm. (b) Quantification of invasive cells. The invasive cells were counted in 10 different fields, and the average was calculated. Data were presented as mean ± SEM. (D) The protein expression levels of MMP2 and MMP9 were determined with western blotting assay at 24 and 48 h after drug treatment. The gray value of each strip was detected by Image J software. β-Actin acted as an internal control. Standardized data were shown as mean ± SEM.

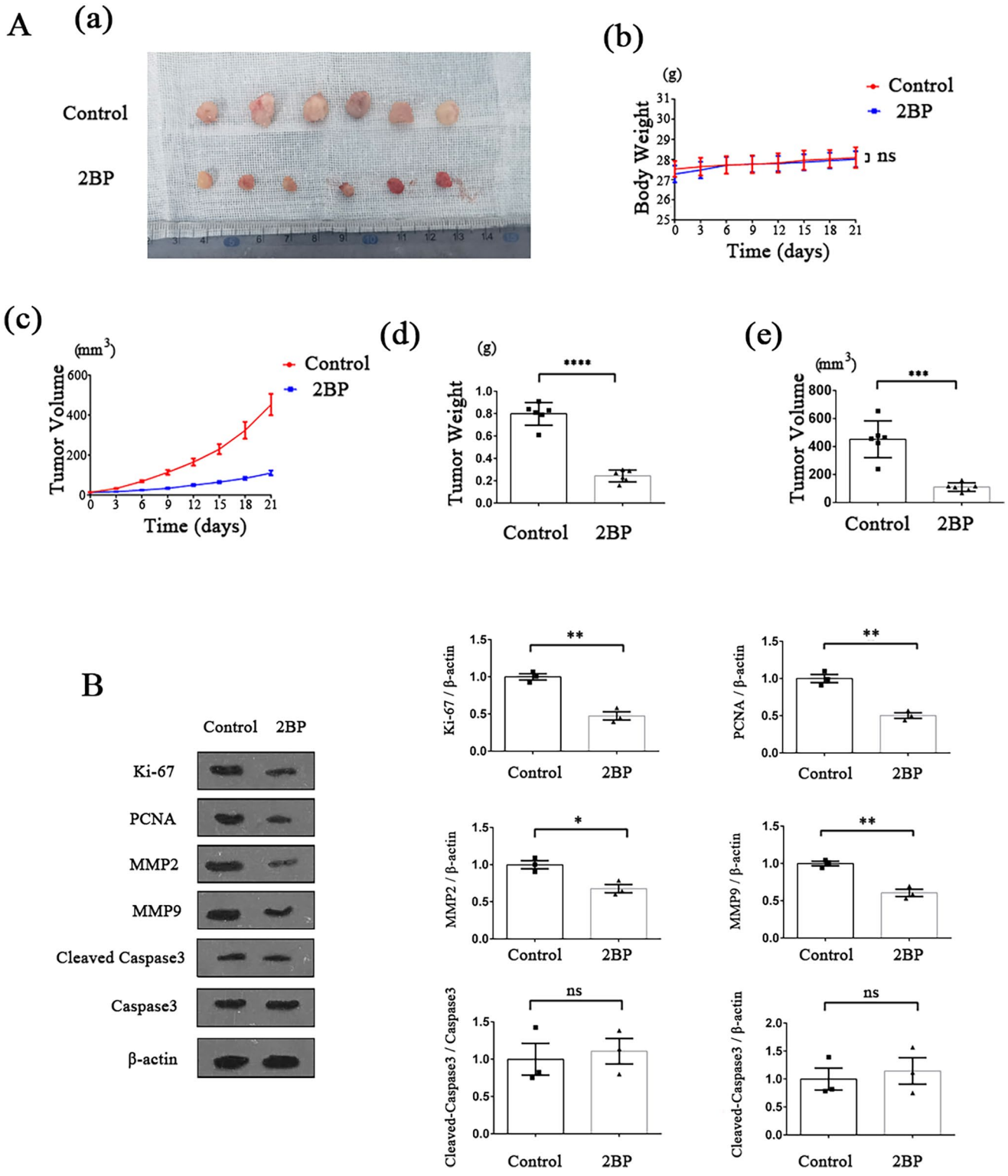

Figure 5. Effect of 2BP on HPSCC cells in nude mouse xenograft model. HPSCC nude mouse xenograft model was established, and the effect of 2BP on tumor growth was monitored ($n = 6$ for each group). (A) (a) After 21-day drug treatment period, tumors were resected and photographed. (b) The body weight of the nude mice was measured every 3 days, and the weight-time curves were shown. Within 21-day drug treatment period, there was no significant difference in body weight between the 2BP-treated group and the control group. Data were shown as mean ± SEM. (c) The tumor volume of the nude mice was measured every 3 days and the tumor volume-time curves were shown. Data were shown as mean ± SEM. (d) and (e) After 21-day drug treatment period, nude mice were executed and tumors were resected. The volume and weight of tumors were measured. Data were shown as mean ± SEM. (B) The protein expression levels of Ki-67, PCNA, MMP2, MMP9, and cleaved-caspase3 in the resected tumors of 2BP-treated group and control group were determined with western blotting assay. The gray value of each strip was detected by Image J software. For Ki-67, PCNA, MMP2, and MMP9, β-actin acted as an internal control. For cleaved-caspase3, capases3, and β-actin acted as internal control, respectively. Standardized data were shown as mean ± SEM.

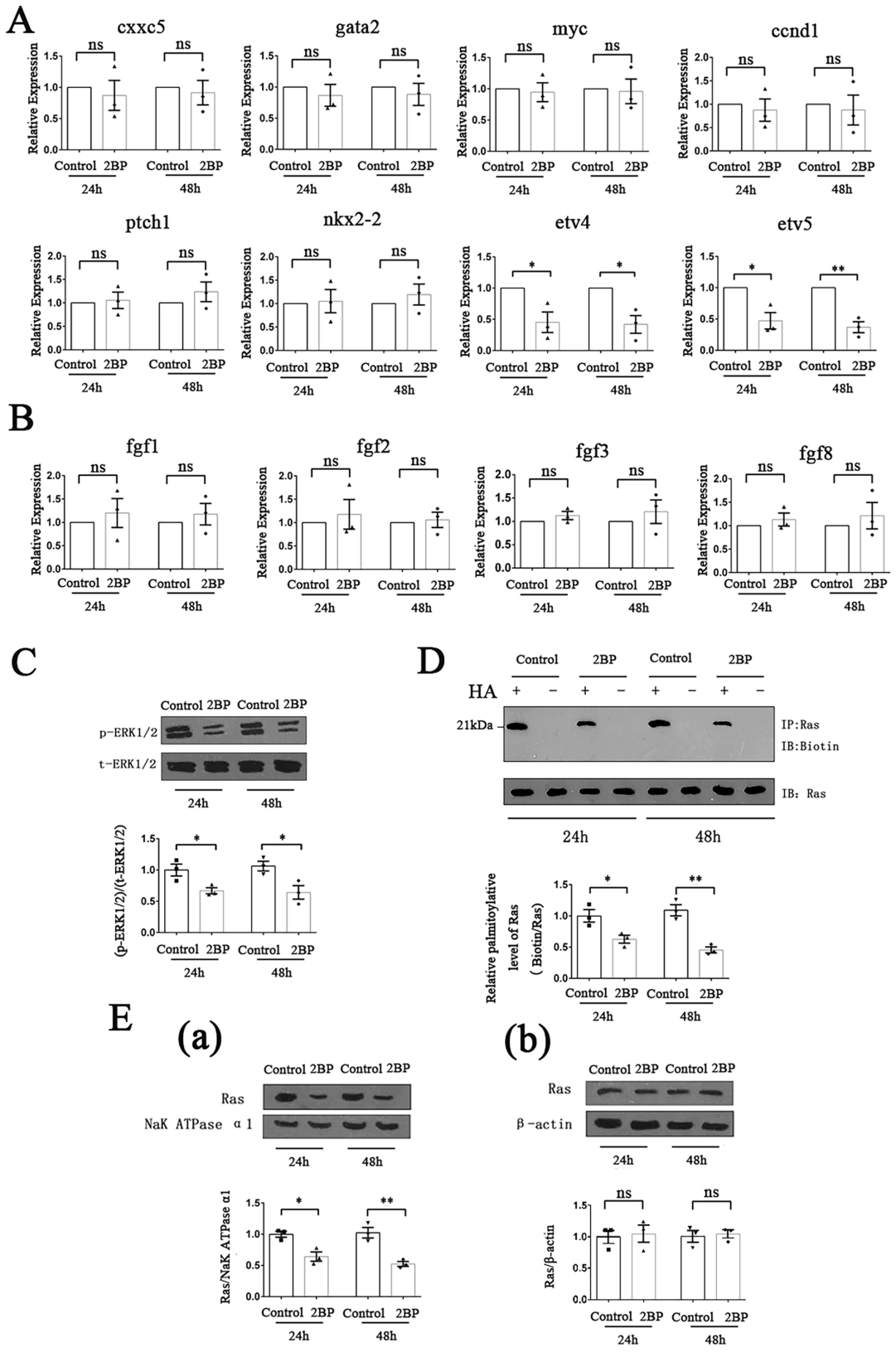

Figure 6. 2BP interfered with FGF/ERK signaling transduction by suppressing the palmitoylation of Ras protein and hindering its membrane localization. HPSCC cells were treated with or without 50 μM 2BP for 24 and 48 h. (A) Transcription levels of *cxxc5*, *gata2*, *myc*, *ccnd1*, *ptch1*, *nkx2-2*, *etv4*, and *etv5* were detected with qRT-PCR. β-Actin acted as an internal control. Data were shown as mean ± SEM. (B) Transcription levels of *fgf1*, *fgf2*, *fgf3*, and *fgf8* were detected with qRT-PCR. β-Actin acted as an internal control. Data were shown as mean ± SEM. (C) Protein level of p-ERK1/2 were determined with western blotting assay. The gray value of each strip was detected by Image J software. t-ERK1/2 acted as an internal control. Standardized data were shown as mean ± SEM. (D) The palmitoylation level of Ras protein was detected using the ABE method. Palmitoylated Ras protein was labeled with biotin and then determined. Total Ras protein served as internal control. Standardized data were shown as mean ± SEM. (E) 2BP hindered the membrane localization of Ras protein. (a) Membrane proteins of HPSCC cells were extracted and the protein level of Ras was determined with western blotting assay. The gray value of each strip was detected by Image J software. NaK ATPase α1 served as an internal control. Standardized data were shown as mean ± SEM. (b) Total proteins of HPSCC cells were extracted and the protein level of Ras was determined with western blotting assay. The gray value of each strip was detected by Image J software. β-Actin served as an internal control. Standardized data were shown as mean ± SEM.

transduction process, and found that there were important sites of protein palmitoylation in Ras protein.[25] So, we detected the palmitoylation level of Ras protein in 50 μM 2BP-treated Fadu cells using ABE method. The results showed that after 2BP treatment for 24 and 48 h, the palmitoylation level of Ras protein in Fadu cells was significantly lower than that of the control group (Figure 6(D)). Protein palmitoylation mainly affects the lipophilicity of proteins, which in turn can affect their binding to cell membrane structure. Considering that Ras protein was an important membrane binding protein, we extracted the total protein and membrane protein of Fadu cells separately, and measured the content of Ras protein using western blotting method. Compared with the control group, the content of Ras protein in the total protein of 2BP-treated group was not significantly different, while the content of Ras protein in the membrane protein was significantly reduced (Figure 6(E)).

Discussion

Modification of protein is a pivotal step before it exerts biological function, among which lipid modification is a very important form. Currently, palmitoylation is the only reversible lipid modification in cells, which can regulate the structure, transport, and localization of proteins, thereby regulating their physiological roles in the body. So far, 23 DHHC proteins have been found in mammals, which can mediate protein palmitoylation. In the past decade, it has been proved that several members of the DHHC protein family are closely related to the specific behavior of stem cells, such as proliferation and differentiation. Considering the high consistency in molecular expression and biological performance between stem cells and tumor cells, the role of these members in tumor occurrence and development is gradually receiving attention. Available data have shown that several DHHC proteins are highly expressed in certain kinds of cancers, which are related to the prognosis, survival rate and treatment outcome of patients.[17,26–28] In this study, we detected the expression of all 23 DHHC protein members in tumor tissues of HPSCC patients, and found that the mRNA and protein levels of DHHC9 and DHHC15 were higher than those in normal hypopharyngeal mucosa. Previous researches have reported that high transcription levels of DHHC9 are an unfavorable prognostic marker in leukemia,[27] and DHHC15 is related to the progression of glioblastoma.[17] For the first time, our study found that these two PAT enzymes were highly expressed in HPSCC, indicating that the protein palmitoylation mediated by them might play an important role in the occurrence and development of hypopharyngeal cancer. They are also expected to become specific molecular markers related to palmitoylation for diagnosis of HPSCC.

Although multiple members of the DHHC protein family were involved in different types of tumor tissues, there were still few reports on the therapeutic modality for tumor based on protein palmitoylation. At present, there is also no ideal chemotherapy drug for HPSCC, with high mortality and poor prognosis. Currently, 2BP is almost the only drug tool to inhibit palmitoylation of proteins. As the molecular weight of 2BP is only 335.3, which is conducive to its absorption and diffusion in organisms, it is widely used in basic medical and biochemical experiments.[29] As yet, a few studies have attempted to apply 2BP to the treatment of disease, such as glucose metabolic disorders and toxoplasma dondii infection.[9,30] In this work, we demonstrated from *in vitro* study that 2BP could arrest the cell cycle of Fadu cells in the G0/G1 phase at a concentration of 50 μM, inhibit cell proliferation, but does not increase cell apoptosis, indicating that it has a significant anti-cancer effect with low cytotoxicity. Besides, we also found that 2BP significantly inhibited invasive and migrational ability of Fadu cells at the same concentration. Consistent with the *in vitro* experiment, our experiments with the HPSCC nude mouse xenograft model also found that administration of 2BP at the concentration of 50 μM/kg significantly decreased the expression of markers for proliferation, invasion and migration in the subcutaneous tumors, while, did not significantly change the activation level of caspase-3, revealing that 2BP could significantly inhibit the growth and progression of HPSCC *in vivo.* Taken together, both *in vitro* and *in vivo* experiments show that 2BP can inhibit the malignant biological behaviors of HPSCC cells without increasing apoptosis, which is expected to be developed as an anti-HPSCC drug with low toxicity and low side effects.

It has been confirmed that tumor proliferation, migration, and invasion are comprehensively regulated by the complex signal transduction network, whose classic components include BMP signaling pathway,[31] Wnt signaling pathway,[32] Shh signaling pathway,[33] FGF signaling pathway,[34] etc. In the present study, we found that 2BP had no significant effect on the transcription levels of the target genes of BMP signaling pathway (*cxxc5* and *gata2*),[35,36] Wnt signaling pathway (*myc* and *ccnd1*)[37] and Shh pathway (*ptch1* and *nkx2-2*).[38] However, it significantly inhibited the transcription of *etv4* and *etv5*, which were the direct target genes of FGF signaling pathway.[39] At the same time, the expression levels of several activators of FGF signaling pathway (*fgf1*, *fgf2*, *fgf3*, and *fgf8*) that promote growth and metastasis of head and neck squamous cell carcinoma [40–42] were not affected in response to 2BP treatment, thereby implying that 2BP might interfere with the transduction process of FGF signaling pathway. What's more, the activation level of ERK1/2 in Fadu cells was significantly reduced after 2BP treatment, which locked the drug target of 2BP to the upstream proteins of ERK1/2 in the FGF/ERK signaling pathway.[43] Generally, the main physiological function of palmitoylation is to regulate the lipophilicity of proteins, which is also the prerequisite for the tight binding of proteins to cell membranes. Compared with other upstream proteins, Ras protein is an important membrane binding protein, and its molecular structure also contains important palmitoylation sites,[25] so it is the most likely target protein for 2BP action. Our molecular chemistry experiments showed that 2BP treatment inhibited palmitoylation of Ras protein in Fadu cells and reduced its ability to bind to cell membranes. Once the membrane localization of Ras protein was obstructed, the transduction process of signaling pathways involved by Ras was inevitably disrupted, hindering its pro-cancer effect (Figure 7). What's more, previous studies have shown that Ras protein is the substrate of DHHC9,[44] which is proved to be highly expressed in HPSCC tissues in

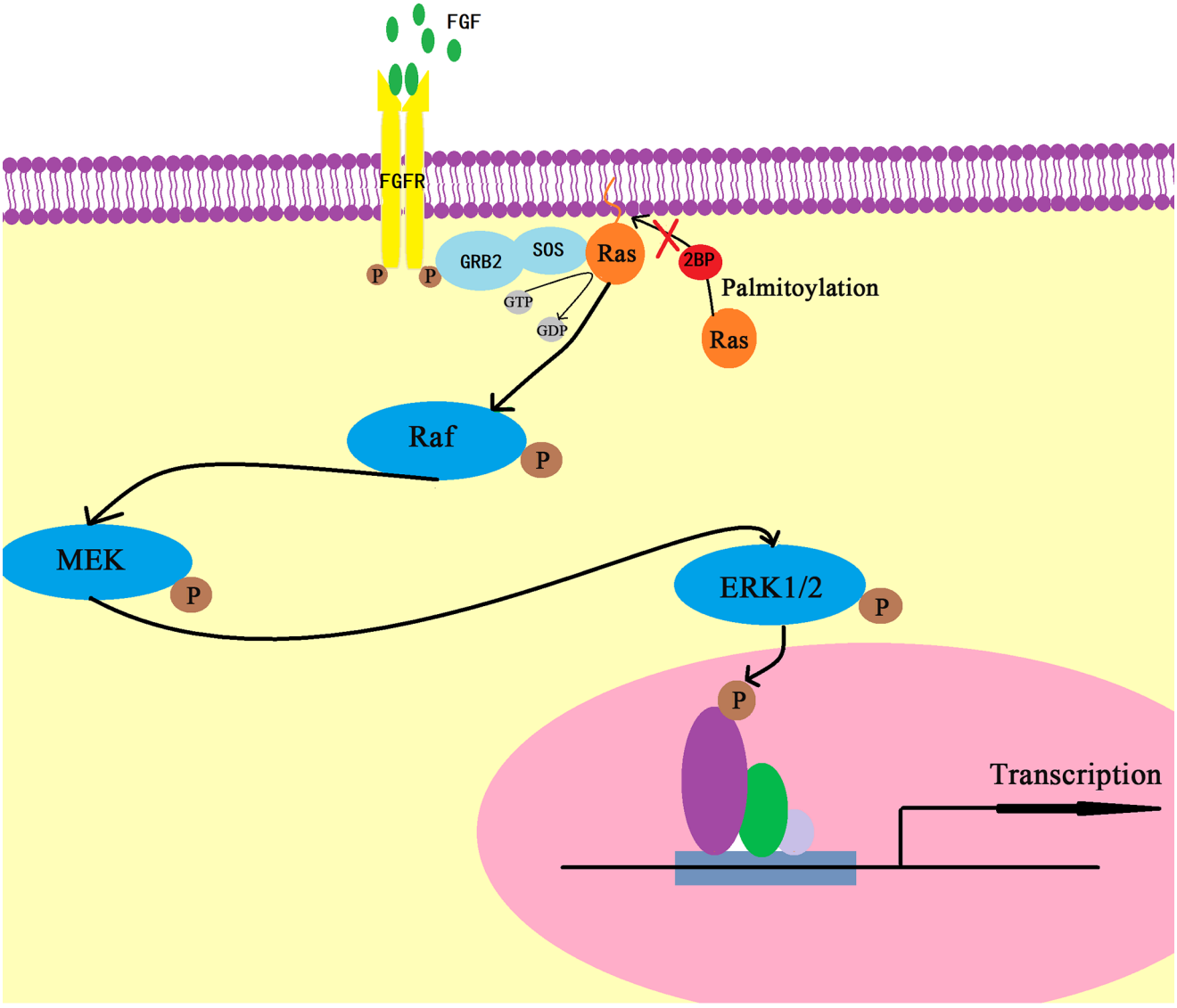

Figure 7. Schematic diagram of underlying molecular mechanism.

this study. So, 2BP is most likely to inhibit DHHC9-mediated palmitoylation to produce anti-tumor effects. In fact, Ras is an important oncogene. Currently, a variety of Ras inhibitors have been used for tumor prevention and treatment.[45] However, our study proved that 2BP exerted anti-cancer effects from the perspective of Ras protein modification and membrane localization, which is a new direction for anti-cancer therapy targeting Ras proteins.

In summary, our experiment shows, for the first time, that protein acyltransferase DHHC9 and DHHC15 are highly expressed in HPSCC tissues. At appropriate concentration, 2BP is able to inhibit the malignant biological behaviors of HPSCC cells, possibly via hindering the palmitoylation and membrane location of Ras protein. From a new perspective of mechanism, 2BP is expected to be developed as a low-toxicity anti-HPSCC drug targeting Ras palmitoylation and membrane localization.

AUTHORS' CONTRIBUTIONS

CZY, WCZ, YZY, WXT, LYQ, and LCL collected clinical specimens and patients' information. CHY maintained the mice. WC and DXG cultured cells and carried out cellular and molecular biological experiments. WC analyzed the data and prepared figures. WC and DXG wrote the initial draft, and LJF edited the manuscript. All authors read the article and approved it for publication.

DECLARATION OF CONFLICTING INTERESTS

The author(s) declared no potential conflicts of interest with respect to the research, authorship, and/or publication of this article.

ETHICAL APPROVAL

Tissue samples were obtained for research with patients' consent. This study was approved by the Research Ethics Committee of Shandong Provincial Hospital.

FUNDING

The author(s) disclosed receipt of the following financial support for the research, authorship, and/or publication of this article: This work was supported in part by the National Natural Science Foundation of China (No. 82071039; No. 81072200)

ORCID ID

Jian-Feng Li https://orcid.org/0000-0002-8542-5424

REFERENCES

1. Wang S, Osgood AO, Chatterjee A. Uncovering post-translational modification-associated protein-protein interactions. *Curr Opin Struct Biol* 2022;**74**:102352
2. Taro C, Takahisa F. Post-translational modification enzymes as key regulators of ciliary protein trafficking. *J Biochem* 2021;**169**:633–42
3. Won SJ, Martin BR. Temporal profiling establishes a dynamic S-palmitoylation cycle. *ACS Chem Biol* 2018;**13**:1560–8
4. Zhang M, Zhou L, Xu Y, Yang M, Xu Y, Komaniecki GP, Kosciuk T, Chen X, Lu X, Zou X, Linder ME, Lin H. A STAT3 palmitoylation cycle promotes TH17 differentiation and colitis. *Nature* 2020;**586**:434–9
5. Jiang H, Zhang X, Chen X, Aramsangtienchai P, Tong Z, Lin H. Protein lipidation: occurrence, mechanisms, biological functions, and enabling technologies. *Chem Rev* 2018;**118**:919–88
6. Lanyon-Hogg T, Faronato M, Serwa RA, Tate EW. Dynamic protein acylation: new substrates, mechanisms, and drug targets. *Trends Biochem Sci* 2017;**42**:566–81
7. Fukata Y, Bredt DS, Fukata M. *Protein palmitoylation by DHHC protein family*. Boca Raton, FL: Taylor & Francis 2006
8. Gelhaus S, Thaa B, Eschke K, Veit M, Schwegmann-Weßels C. Palmitoylation of the Alphacoronavirus TGEV spike protein S is essential for incorporation into virus-like particles but dispensable for S-M interaction. *Virology* 2014;**464–465**:397–405
9. Alonso AM, Coceres VM, De Napoli MG, Nieto Guil AF, Angel SO, Corvi MM. Protein palmitoylation inhibition by 2-bromopalmitate alters gliding, host cell invasion and parasite morphology in Toxoplasma gondii. *Mol Biochem Parasitol* 2012;**184**:39–43
10. Chen X, Shi W, Wang F, Du Z, Yang Y, Gao M, Yao Y, He K, Wang C, Hao A. Zinc finger DHHC-type containing 13 regulates fate specification of ectoderm and mesoderm cell lineages by modulating Smad6 activity. *Stem Cells Dev* 2014;**23**
11. Shi W, Chen X, Wang F, Gao M, Yang Y, Du Z, Wang C, Yao Y, He K, Hao A. ZDHHC16 modulates FGF/ERK dependent proliferation of neural stem/progenitor cells in the zebrafish telencephalon. *Dev Neurobiol* 2016;**76**:1014–28
12. Fan X, Yang H, Hu L, Wang D, Wang R, Hao A, Chen X. Propofol impairs specification of retinal cell types in zebrafish by inhibiting Zisp-mediated Noggin-1 palmitoylation and trafficking. *Stem Cell Res Ther* 2021;**12**:195
13. Wang F, Chen X, Shi W, Yao L, Gao M, Yang Y, Hao A. Zdhhc15b regulates differentiation of diencephalic dopaminergic neurons in zebrafish. *J Cell Biochem* 2015;**116**:2980–91
14. Liu F, Yang H, Zhang X, Sun X, Zhou J, Li Y, Liu Y, Zhuang Z, Wang G. Inhibition of Musashi-1 enhances chemotherapeutic sensitivity in gastric cancer patient-derived xenografts. *Exp Biol Med* 2022;**247**:868–79
15. Yin W, Wang J, Jiang L, James Kang Y. Cancer and stem cells. *Exp Biol Med* 2021;**246**:1791–801
16. Greenlee JD, Lopez-Cavestany M, Ortiz-Otero N, Liu K, Subramanian T, Cagir B, King MR. Oxaliplatin resistance in colorectal cancer enhances TRAIL sensitivity via death receptor 4 upregulation and lipid raft localization. *Elife* 2021;**10**:e67750
17. Fan X, Yang H, Zhao C. Local anesthetics impair the growth and self-renewal of glioblastoma stem cells by inhibiting ZDHHC15-mediated GP130 palmitoylation. *Stem Cell Res Ther* 2021;**12**:107
18. Chen S, Zhu B, Yin C, Liu W, Han C, Chen B, Liu T, Li X, Chen X, Li C, Hu L, Zhou J, Xu ZX, Gao X, Wu X, Goding CR, Cui R. Palmitoylation-dependent activation of MC1R prevents melanomagenesis. *Nature* 2017;**549**:399–403
19. Lan T, Delalande C, Dickinson BC. Inhibitors of DHHC family proteins. *Curr Opin Chem Biol* 2021;**65**:118–25
20. Petersen JF, Timmermans AJ, van Dijk BAC, Overbeek LIH, Smit LA, Hilgers FJM, Stuiver MM, van den Brekel MWM. Trends in treatment, incidence and survival of hypopharynx cancer: a 20-year population-based study in the Netherlands. *Eur Arch Otorhinolaryngol* 2018;**275**:181–9
21. Suzuki M, Fujii T, Yoshii T, Otozai S, Kitamura K, Kanamura R, Omori Y, Minamino T. Trends in the detail of the stage and survival rate in hypopharyngeal cancer over 20 years. *Nihon Jibiinkoka Gakkai Kaiho* 2016;**119**:949–54
22. Yu P, Wu R, Zhou Z, Zhang X, Wang R, Wang X, Lin S, Wang J, Lv L. rAj-Tspin, a novel recombinant peptide from Apostichopus japonicus, suppresses the proliferation, migration, and invasion of BEL-7402 cells via a mechanism associated with the ITGB1-FAK-AKT pathway. *Invest New Drugs* 2021;**39**:377–85
23. Chen X, Du Z, Shi W, Wang C, Yang Y, Wang F, Yao Y, He K, Hao A. 2-Bromopalmitate modulates neuronal differentiation through the regulation of histone acetylation. *Stem Cell Res* 2014;**12**:481–91
24. Liu Q, Li G, Li R, Shen J, He Q, Deng L, Zhang C, Zhang J. IL-6 promotion of glioblastoma cell invasion and angiogenesis in U251 and T98G cell lines. *J Neurooncol* 2010;**100**:165–76
25. Busquets-Hernández C, Triola G. Palmitoylation as a key regulator of ras localization and function. *Front Mol Biosci* 2021;**8**:659861
26. Peng C, Zhang Z, Wu J, Lv Z, Tang J, Xie H, Zhou L, Zheng S. A critical role for ZDHHC2 in metastasis and recurrence in human hepatocellular carcinoma. *Biomed Res Int* 2014;**2014**:832712–9
27. Liu P, Jiao B, Zhang R, Zhao H, Zhang C, Wu M, Li D, Zhao X, Qiu Q, Li J, Ren R. Palmitoylacyltransferase Zdhhc9 inactivation mitigates leukemogenic potential of oncogenic Nras. *Leukemia* 2016;**30**:1225–8
28. Dzikiewicz-Krawczyk A, Kok K, Slezak-Prochazka I, Robertus JL, Bruining J, Tayari MM, Rutgers B, de Jong D, Koerts J, Seitz A, Li J, Tillema B, Guikema JE, Nolte IM, Diepstra A, Visser L, Kluiver J, van den Berg A. ZDHHC11 and ZDHHC11B are critical novel components of the oncogenic MYC-miR-150-MYB network in Burkitt lymphoma. *Leukemia* 2017;**31**:1470–3
29. Zheng B, DeRan M, Li X, Liao X, Fukata M, Wu X. 2-Bromopalmitate analogues as activity-based probes to explore palmitoyl acyltransferases. *J Am Chem Soc* 2013;**135**:7082–5
30. Mohammed AM, Syeda K, Hadden T, Kowluru A. Upregulation of phagocyte-like NADPH oxidase by cytokines in pancreatic beta-cells: attenuation of oxidative and nitrosative stress by 2-bromopalmitate. *Biochem Pharmacol* 2013;**85**:109–14
31. Blanco Calvo M, Bolós Fernández V, Medina Villaamil V, Aparicio Gallego G, Díaz Prado S, Grande Pulido E. Biology of BMP signalling and cancer. *Clin Transl Oncol* 2009;**11**:126–37
32. Parsons MJ, Tammela T, Dow LE. WNT as a driver and dependency in cancer. *Cancer Discov* 2021;**11**:2413–29
33. Jiang J. Hedgehog signaling mechanism and role in cancer. *Semin Cancer Biol* 2022;**85**:107–22
34. Liu G, Chen T, Ding Z, Wang Y, Wei Y, Wei X. Inhibition of FGF-FGFR and VEGF-VEGFR signalling in cancer treatment. *Cell Prolif* 2021;**54**:e13009
35. Kim HY, Yang DH, Shin SW, Kim MY, Yoon JH, Kim S, Park HC, Kang DW, Min D, Hur MW, Choi KY. CXXC5 is a transcriptional activator of Flk-1 and mediates bone morphogenic protein-induced endothelial cell differentiation and vessel formation. *FASEB J* 2014;**28**:615–26
36. Ferri-Lagneau KF, Moshal KS, Grimes M, Zahora B, Lv L, Sang S, Leung T. Ginger stimulates hematopoiesis via Bmp pathway in zebrafish. *PLoS ONE* 2012;**7**:e39327
37. Katoh M, Katoh M. WNT signaling and cancer stemness. *Essays Biochem* 2022;**66**:319–31
38. Shahi MH, Afzal M, Sinha S, Eberhart CG, Rey JA, Fan X, Castresana JS. Regulation of sonic hedgehog-GLI1 downstream target genes PTCH1, Cyclin D2, Plakoglobin, PAX6 and NKX2.2 and their epigenetic status in medulloblastoma and astrocytoma. *BMC Cancer* 2010;**10**:614

39. DeSalvo J, Ban Y, Li L, Sun X, Jiang Z, Kerr DA, Khanlari M, Boulina M, Capecchi MR, Partanen JM, Chen L, Kondo T, Ornitz DM, Trent JC, Eid JE. ETV4 and ETV5 drive synovial sarcoma through cell cycle and DUX4 embryonic pathway control. *J Clin Invest* 2021;**131**: e141908
40. Liu Z, Hartman YE, Warram JM, Knowles JA, Sweeny L, Zhou T, Rosenthal EL. Fibroblast growth factor receptor mediates fibroblast-dependent growth in EMMPRIN-depleted head and neck cancer tumor cells. *Mol Cancer Res* 2011;**9**:1008–17
41. Jovanovic IP, Radosavljevic GD, Simovic-Markovic BJ, Stojanovic SP, Stefanovic SM, Pejnovic NN, Arsenijevic NN. Clinical significance of Cyclin D1, FGF3 and p21 protein expression in laryngeal squamous cell carcinoma. *J BUON* 2014;**19**:944–52
42. Hao Y, Xiao Y, Liao X, Tang S, Xie X, Liu R, Chen Q. FGF8 induces epithelial-mesenchymal transition and promotes metastasis in oral squamous cell carcinoma. *Int J Oral Sci* 2021;**13**:6
43. Soszyńska A, Klimczewska K, Suwińska A. FGF/ERK signaling pathway: how it operates in mammalian preimplantation embryos and embryo-derived stem cells. *Int J Dev Biol* 2019;**63**:171–86
44. Swarthout JT, Lobo S, Farh L, Croke MR, Greentree WK, Deschenes RJ, Linder ME. DHHC9 and GCP16 constitute a human protein fatty acyltransferase with specificity for H- and N-Ras. *J Biol Chem* 2005;**280**:31141–8
45. Awad MM, Liu S, Rybkin II, Arbour KC, Dilly J, Zhu VW, Johnson ML, Heist RS, Patil T, Riely GJ, Jacobson JO, Yang X, Persky NS, Root DE, Lowder KE, Feng H, Zhang SS, Haigis KM, Hung YP, Sholl LM, Wolpin BM, Wiese J, Christiansen J, Lee J, Schrock AB, Lim LP, Garg K, Li M, Engstrom LD, Waters L, Lawson JD, Olson P, Lito P, Ou SI, Christensen JG, Jänne PA, Aguirre AJ. Acquired resistance to KRASG12C inhibition in cancer. *N Engl J Med* 2021;**384**:2382–93

(Received August 18, 2023, Accepted October 16, 2023)